THE JOURNAL OF BIOLOGICAL CHEMISTRY VOL. 286, NO. 15, pp. 13638–13646, April 15, 2011

Endoplasmic Reticulum Stress-induced Apoptosis in *Leishmania* through Ca^{2+}-dependent and Caspase-independent Mechanism*[S]

Received for publication, November 9, 2010, and in revised form, February 10, 2011 Published, JBC Papers in Press, February 17, 2011, DOI 10.1074/jbc.M110.201889

Subhankar Dolai[1], **Swati Pal**[1], **Rajesh K. Yadav, and Subrata Adak**[2]

From the Division of Structural Biology and Bio-informatics, Indian Institute of Chemical Biology, 4, Raja S.C. Mullick Road, Kolkata-700 032, India

Numerous reports have shown that mitochondrial dysfunctions play a major role in apoptosis of *Leishmania* parasites, but the endoplasmic reticulum (ER) stress-induced apoptosis in *Leishmania* remains largely unknown. In this study, we investigate ER stress-induced apoptotic pathways in *Leishmania major* using tunicamycin as an ER stress inducer. ER stress activates the expression of ER-localized chaperone protein BIP/GRP78 (binding protein/identical to the 78-kDa glucose-regulated protein) with concomitant generation of intracellular reactive oxygen species. Upon exposure to ER stress, the elevation of cytosolic Ca^{2+} level is observed due to release of Ca^{2+} from internal stores. Increase in cytosolic Ca^{2+} causes mitochondrial membrane potential depolarization and ATP loss as ablation of Ca^{2+} by blocking voltage-gated cation channels with verapamil preserves mitochondrial membrane potential and cellular ATP content. Furthermore, ER stress-induced reactive oxygen species (ROS)-dependent release of cytochrome *c* and endonuclease G from mitochondria to cytosol and subsequent translocation of endonuclease G to nucleus are observed. Inhibition of caspase-like proteases with the caspase inhibitor benzyloxycarbonyl-VAD-fluoromethyl ketone or metacaspase inhibitor antipain does not prevent nuclear DNA fragmentation and phosphatidylserine exposure. Conversely, significant protection in tunicamycin-induced DNA degradation and phosphatidylserine exposure was achieved by either pretreatment of antioxidants (*N*-acetyl-L-cysteine, GSH, and L-cysteine), chemical chaperone (4-phenylbutyric acid), or addition of Ca^{2+} chelator (1,2-bis(2-aminophenoxy)ethane-*N,N,N,N*-tetraacetic acid-acetoxymethyl ester). Taken together, these data strongly demonstrate that ER stress-induced apoptosis in *L. major* is dependent on ROS and Ca^{2+}-induced mitochondrial toxicity but independent of caspase-like proteases.

Limited programmed cell death in *Leishmania* prior to infection plays a crucial role in disease establishment (1–3). *Leishmania* undergoes apoptotic cell death upon treatment with antimony, camptothecin, H_2O_2, or antimicrobial peptides (4–7). Cytosolic calcium-mediated mitochondrial toxicity, activation of caspase-3/7-like protease, and release of mitochondrial apoptotic factors have been implicated in these processes. Many reports have been established that *Leishmania* can undergo apoptosis in both caspase-dependent and caspase-independent pathways (8–10) during mitochondrial oxidative stress, but still nothing is known regarding endoplasmic reticulum (ER)[3] stress-induced apoptosis in *Leishmania*.

The ER is a multifunctional organelle in cells where the important steps in the folding and modification of proteins as well as the selection for transport to other compartments occur (11, 12). The ER also plays important role in calcium (Ca^{2+}) signaling regulation, vesicle trafficking, drug metabolism, and lipid biogenesis (13, 14). Again, this organelle can initiate apoptosis when it encounters the accumulation of unfolded proteins or the inhibition of the ER-Golgi transport (15). Three ER-resident transmembrane proteins, inositol-requiring enzyme 1 (IRE1), PKR-like ER kinase (PERK), and the basic leucine-zipper transcription factor 6 (ATF-6), have been identified as the proximal sensors of ER stress. Several groups of workers have established that the ER responds to stress through decreasing protein translation with the activation of PERK signaling, up-regulation of ER-resident chaperone proteins through ATF-6, and the activation of ER-specific protein-degrading apparatus by IRE1-signaling proteins to minimize the accumulation of unfolded proteins, which is collectively known as the unfolded protein response (UPR) (16). The activation of the UPR causes the up-regulation of the genes that encode ER chaperone proteins such as Bip/GRP78, which increases the protein folding activity and prevents protein aggregation (17). However, it is reported that the accumulation of misfolded proteins within the lumen of the ER can lead to prolonged UPR activation, which in turn causes oxidative stress, resulting eventually in cell death (18, 19).

Tunicamycin (TM), a naturally occurring antibiotic, can induce ER stress by inhibiting the first step in the biosynthesis

* This work was supported by Council of Scientific and Industrial Research Project NWP 0038 and Council of Scientific and Industrial Research fellowships (to S. D., R. K. Y., and S. P.).

[S] The on-line version of this article (available at http://www.jbc.org) contains supplemental Fig. S1.

[1] Both authors contributed equally to this work.

[2] To whom correspondence should be addressed. Tel.: 91-33-2473-6793; Fax: 91-33-2473-5197; E-mail: adaks@iicb.res.in.

[3] The abbreviations used are: ER, endoplasmic reticulum; TM, tunicamycin; BiP, binding protein; PBA, 4-phenylbutyric acid; H_2DCFDA, 2′,7′-dichlorodihydrofluorescein diacetate, acetyl ester; Endo G, endonuclease G; NAC, *N*-acetyl-L-cysteine; PI, propidium iodide; ROS, reactive oxygen species; Z, benzyloxycarbonyl; FMK, fluoromethyl ketone; Boc, *t*-butyloxycarbonyl; AMC, amido-4-methylcoumarin; BAPTA-AM, 1,2-bis(2-aminophenoxy)ethane-*N,N,N,N*-tetraacetic acid-acetoxymethyl ester; CCCP, carbonyl cyanide 3-chlorophenylhydrazone; Cyt *c*, cytochrome *c*; MTT, 3-(4,5-dimethylthiazol-2-yl)-2,5-diphenyl tetrazolium bromide; PS, phosphatidylserine; UPR, unfolded protein response.

of *N*-linked oligosaccharides within cells (20). Many reports suggest that TM can induce apoptosis in different cell lines (21, 22). It has been previously shown that TM inhibits the growth and infectivity of *Leishmania mexicana amazonensis* (23), *Leishmania braziliensis* (24), and *Leishmania donovani* (25). However, the potential roles of TM in ER stress and UPR-mediated execution of apoptosis in *Leishmania* have not been explored to date. The absence of genes like caspases, homologues of the mammalian Bcl-2 protein family, and the ER stress-induced apoptotic protein components indicates that the *Leishmania* programmed cell death pathway differs from that of typical mammalian apoptosis, making it an interesting subject of investigation.

In this study, we have established the mechanism of ER stress-induced apoptotic cell death in *Leishmania.* We have shown that the TM-induced ER stress results in dramatic increments in both ROS and cytosolic Ca^{2+} concentration in *Leishmania*, which is responsible for alterations in the mitochondrial membrane function and finally leads to cell death. This phenomenon is abrogated by blockade of calcium release as well as antioxidant pretreatment. Although the blockade of caspase proteases influences slightly influenced in ameliorating DNA degradation, it does not prevent cell death, suggesting that TM-induced apoptosis is a caspase-independent process. Taken together, our results unlock the mechanistic pathway of ER stress-induced apoptosis in *Leishmania* cells. These data also provide a framework for understanding the critical events in ER stress-mediated apoptosis and suggest that *Leishmania* programmed cell death pathway differs from that of typical mammalian apoptosis.

EXPERIMENTAL PROCEDURES

Reagents—Mitoprobe^{TM} JC-1 assay kit for flow cytometry, Fluo 4-AM, Pluronic F127, MitoSOX^{TM} Red, BAPTA-AM, calcium ionophore A23187, and fetal bovine serum were purchased from Molecular Probes (Eugene, OR). TM, 4-phenylbutyric acid (PBA), H_2DCFDA, antipain, verapamil, and 3-(4,5-dimethylthiazol-2-yl)-2,5-diphenyl tetrazolium bromide (MTT) were procured from Sigma. Caspase-12 assay kit and caspase-12 inhibitor Z-ATAD-FMK were obtained from Biovision. Caspase-3/7 inhibitor Z-VAD-FMK and terminal deoxynucleotidyltransferase enzyme-mediated dUTP nick end-labeling (TUNEL) assay kit were procured from Clontech. The fluorogenic substrate *t*-butyloxycarbonyl-Gly-Arg-Arg-7-amido-4-methylcoumarin (Boc-GRR-AMC) was purchased from Bachem (Bubendorf, Switzerland). All other chemicals, unless specified, were obtained from Sigma or sources mentioned previously (26–28).

Parasite Culture and Treatment—Promastigote form of *L. major* (5ASKH) was cultured in M199 media supplemented with 10% heat-inactivated fetal bovine serum as described previously (26–28). TM was dissolved in anhydrous dimethyl sulfoxide (DMSO) at 10 mg/ml. Exponentially growing promastigotes (5×10^6 cells/ml) in the complete medium were treated with 20 μg/ml TM to induce apoptosis. Control cells were treated with 0.2% DMSO in each experiment. Voltage-gated channel blocker verapamil was added at a 10 μM concentration 1 h prior the addition of TM to the cells. Z-VAD-FMK was used at 50 μM final concentration. Final concentration of NAC, GSH, L-cysteine, PBA, and BAPTA-AM were 20, 0.5, 20, and 2.0 mM and 100 μM, respectively.

Parasite Survival Assay—Viability of *L. major* during ER stress was measured by MTT (Sigma) as described previously (27). Exponentially growing promastigotes (2×10^6) in M199 media were exposed to different concentrations of TM for 2.0 to 16.0 h. After treatment cells were washed with ice-cold 1× PBS and incubated in fresh M199 media with 10% heat-inactivated FBS and 0.5 mg/ml MTT for 3 h. After 3 h, cells were pelleted by centrifugation (1200 × *g* for 5.0 min). After washing twice with 1× PBS, 100 μl of 0.04 N HCl in isopropyl alcohol was added. The absorbance of these solutions was measured on a microplate reader at 570 nm. The percentage of viability was calculated from OD readings. All experiments were performed in triplicate. Viability assay showed that 95% of cellular death had taken place in *L. major* promastigotes by 16 h of treatment with 20 μg/ml TM.

Detection of ROS—To detect endogenous ROS production, control or TM-treated *L. major* promastigotes (1×10^7 cells/ml) were incubated with 10 μM peroxide-sensitive fluorescent probe 2′,7′-dichlorodihydrofluorescein diacetate acetyl ester (H_2DCFDA) for 30 min at 26 °C in the dark with mild shaking. In the presence of intracellular H_2O_2, nonfluorescent membrane-permeable H_2DCFDA converted to impermeable fluorogenic 2′,7′-dichlorofluorescein. ROS production was thus monitored by measuring 2′,7′-dichlorofluorescein emission at 530 nm with excitation at 488 nm for 1 h using a spectrofluorimeter. Generation of mitochondrial ROS was monitored by flow cytometry with the mitochondrion-specific ROS-detecting probe MitoSOX^{TM} Red as described previously (26).

Ca^{2+} Analysis—Intracellular free Ca^{2+} concentrations were measured using Ca^{2+}-specific fluorescent probe Fluo-4/AM (Molecular Probes, Eugene, OR) as described previously with minor modifications (27). 1×10^7 cells/ml parasites were loaded with 6.0 μM Fluo-4/AM for 60 min at room temperature in the presence of 5 μM pluronic acid F127. After incubation, cells were harvested and washed twice with fresh serum-free medium and analyzed with a fluorescence spectrophotometer. Time-dependent emission kinetics at 518 nm (excitation at 488 nm) were performed to detect the time-dependent cytosolic release of intracellular stored Ca^{2+} immediately after the addition of TM. Quantification of free cytosolic Ca^{2+} was calculated using the following formula: $[Ca^{2+}]_c = K_d\,(F - F_{min})/(F_{max} - F)$, where K_d is 345 nM; F indicates fluorescence intensity of the cells; F_{min} indicates minimum fluorescence of the cells obtained by treating cells with 10 μM calcium ionophore (A2308) in the presence of 3 mM EGTA; and F_{max} indicates maximum fluorescence of cells achieved in the presence of calcium ionophore and 10 mM $CaCl_2$. Measurement of intracellular Ca^{2+} was also carried out in the presence of Ca^{2+} channel inhibitors. Parasites were incubated with specific voltage-gated channel blocker verapamil (10 μM) for 1 h before addition of TM to the cells.

Mitochondrial Membrane Potential ($\Delta\psi_m$) Measurement—Mitochondrial membrane potential ($\Delta\psi_m$) was assayed by flow cytometry with 5,5′,6,6′-tetrachloro-1,1′,3,3′-tetraethylbenzimidazole carbocyanide iodide (JC-1) as a probe. JC-1 is a cationic and lipophilic vital dye that concentrates to mitochondria

in a potential dependent manner. Measurements were performed according to the manufacturer's instruction. Briefly, after treatment, cells were washed twice and resuspended in 1 ml of PBS at 1×10^6 cells/ml. JC-1 probe was added to 6 μM final concentration and incubated for 20 min at 26 °C. For positive control, 50 μM of the mitochondrial uncoupler, carbonyl cyanide 3-chlorophenylhydrazone (CCCP), was added to non-treated control cells 15 min prior to addition of JC-1. Analysis was performed on FACS Canto flow cytometer (BD Biosciences) equipped with 488-nm excitation and 530/590-nm emission filters for monomeric form and J-aggregate formations, respectively, after appropriate fluorescence compensation. Data were analyzed with FACSDiva software.

Measurement of ATP—Cellular ATP concentration was measured by bioluminescence method using an ATP determination kit (Molecular Probes). Briefly, control and TM-treated cells (1×10^7) were mixed with reaction buffer containing 1 mM DTT, 0.5 mM luciferin, and 12.5 μg/ml luciferase. Luminescence intensity was measured in a luminometer (Promega). ATP concentrations were calculated from the ATP standard curve, and cellular ATP levels were expressed as nmol/10^6 cells.

Subcellular Fractionation and Western Blot Analysis—Subcellular fractionation was performed to separate mitochondria, nuclei, and cytosol by the mitochondria isolation kit (Qiagen). The purity of each fraction was checked by Western blot analysis of the organelle-specific marker antibody. Western blot analysis was performed as described previously (26). The primary antibodies used were as follows: rabbit anti (*Trypanosoma brucei*)-cytochrome *c* antibody (1:500), rabbit anti (*L. donovani*)-Endo G antibody (1:500), mouse anti (*Leishmania tropica*)-mitochondrial RNA import complex I antibody (1:100), rabbit anti (*L. donovani*)-adenosine kinase (1:50), and rabbit anti-(goat) histone H3B antibody (1:1000). The HRP-conjugated secondary antibodies used were anti-rabbit (1:10,000), anti-goat (1:6000), and anti-mouse (1:6000). In each experiment, 50 μg of total protein was loaded as mentioned in each case. Precise quantitation was done by densitometric analysis to calculate the expression of the protein of interest with that of histone H3B, mitochondrial RNA import complex I, or adenosine kinase, which was immunodetected in the same sample. Densitometric analysis was performed by importing images to a personal computer using Total Lab TL 100 software (Nonlinear Dynamics Ltd.).

Apoptosis Assessment by PI and Annexin-V Staining—Phosphatidylserine (PS) exposure was assessed by Vybrant apoptosis assay kit 3 (Molecular Probes). After the incubation with TM, cells were harvested at 4 °C by centrifugation for 5 min at $1200 \times g$ and washed twice with cold 1× PBS. Cells (1×10^6/ml) were then resuspended in 100 μl of 1× annexin binding buffer for 15 min at room temperature. 5 μl of FITC-conjugated annexin V and 1.0 μg/ml PI were further added to the mixture and incubated for another 20 min. After staining, 400 μl of 1× buffer was added to the mixture, and samples were stored on ice until data acquisition by flow cytometry. Measurements were completed within 1 h.

For microscopy, FITC-conjugated annexin V and PI-labeled equivalent cells were adhered to poly-L-lysine-coated slide and visualized with Leica TCS-SP confocal microscope. Cells with annexin V externalization accumulate more FITC dye with emission at 530 nm (green fluorescence, see supplemental Fig. 1).

Caspase-12-like Protease Activity Assay—Caspase-12-like protease activity was measured fluorimetrically using caspase-12-specific substrate, ATAD-AFC (caspase-12 assay kit, Biovision Research Products), as per the manufacturer's instructions. Briefly, after treatment of TM, cells were lysed in lysis buffer, and 300 μg of total protein from each sample was used for the assay. The assay was based on detection of cleavage of substrate ATAD-AFC to free AFC, which was measured by micro-plate reader (emission 400 nm and excitation 505 nm). Caspase-12-specific inhibitor Z-ATAD-FMK (10 μl) was added in control reactions for 30 min before the addition of ER stress inducers.

Detection of Caspase-3/7 and Metacaspase-like Protease Activity—The detection of caspase activity by fluorochrome inhibitor of caspases (a caspase-3- and -7-specific fluorogenic inhibitor, FAM-DEVD-FMK) was based on affinity labeling of the reactive center cysteine residue of activated caspases by the FMK moiety of the fluorochrome inhibitor of caspases via the caspase-specific recognition sequence aspartic acid-glutamic acid-valine-aspartic acid (DEVD) as described previously (27). Caspase inhibitor Z-VAD-FMK was added in control reactions at 50 μM for 30 min prior to the addition of ER stress inducer. Metacaspase-like protease activity was measured fluorimetrically using Boc-GRR-AMC substrate as described by Lee *et al.* with minor modifications (29, 30). Briefly, promastigote cultures were pelleted by centrifugation and resuspended in fresh culture medium containing 20 μg/ml TM, and the sample was incubated for 16 h at 26 °C. 1.0 μM antipain (metacaspase inhibitor) was added in control reactions for 30 min before the addition of the ER stress inducer. Treated or untreated parasites were lysed (10^8 cells/ml) in lysis buffer (50 mM Tris-HCl, pH 7.5, 1% (v/v) Triton X-100, 10% (w/v) sucrose, 150 mM NaCl) for 30 min on ice, and the insoluble material was eliminated by centrifugation at 15,000 × *g* for 20 min at 4 °C. 150 μl of supernatant was incubated with 75 μM fluorogenic substrate (Boc-GRR-AMC), 5 mM DTT, and 10 mM $CaCl_2$ for 2 h at 37 °C under gentle agitation and transferred to a microwell plate. Sample was analyzed immediately with a fluorescence spectrophotometer with excitation at 355 nm and emission at 460 nm. Protease activity was expressed in relative fluorescence units.

TUNEL Staining—In situ DNA fragmentation was analyzed by the terminal deoxyribonucleotide transferase-mediated deoxyuridine triphosphate nick end-labeling (TUNEL assay) kit (Clontech) as described previously (27). Involvement of caspases in DNA degradation was assessed by the addition of caspase inhibitors. Quantification and degree of nicked DNA in a population of parasites were further detected by flow cytometry. Analysis was performed on a flow cytometer equipped with 488-nm excitation and 530/590-nm emission filters for FITC-labeled dUTP and fluorescence, respectively, after appropriate fluorescence compensation. DMSO (0.2%)-treated samples were used as negative control. For microscopy, TUNEL-stained cells were adhered to poly-L-lysine coated slides and visualized with a Leica TCS-SP confocal microscope. TUNEL-

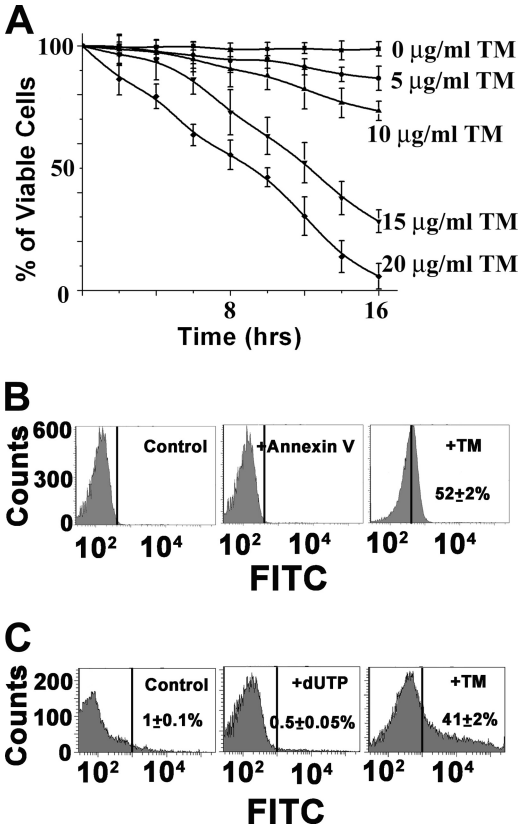

FIGURE 1. **TM induces apoptosis in *L. major*.** *A,* percentage of viable cells after treatment of 0.2% DMSO as control or TM. Promastigotes of *L. major* were treated at the indicated time, and parasite viability was detected by MTT assay. Average and S.D. values were taken from three independent experiments and plotted against time. *B,* flow cytometric analysis of PS externalization in control or TM-treated cells. *C,* TUNEL analysis by flow cytometry.

positive cells accumulate more FITC dye with emission at 530 nm.

Statistical Analysis—All results were expressed as the means ± S.D. from at least three independent experiments. Statistical analysis for parametric data were calculated by Student's *t* test or analysis of variance wherever applicable using Origin 7.0 software (Microcal Software, Inc., Northampton, MA). Analysis of variance was followed by post hoc analysis (multiple comparison *t* test) for the evaluation of the difference between individual groups. A p value of less than 0.05 was considered statistically significant.

RESULTS

TM Induces Programmed Cell Death-like Features through ER Stress in L. major—To analyze the role of ER stressor in parasite viability, we performed a viability test by MTT assay. TM treatment showed dose- and time-dependent loss of parasite viability, and 95% cell death was detected on treatment with 20 μg/ml TM for 16 h (Fig. 1*A*). To assess whether the loss of viability was through apoptotic cell death, we examined DNA fragmentation and PS exposure, two established hallmarks of apoptosis. Flow cytometric analysis revealed extensive (52%) PS externalization in TM-treated cells, although exponentially growing control promastigotes did not have any PS-positive cells (Fig. 1*B*). Similarly, TUNEL assay by flow cytometry indicated about 41% DNA fragmentation (Fig. 1*C*) in comparison

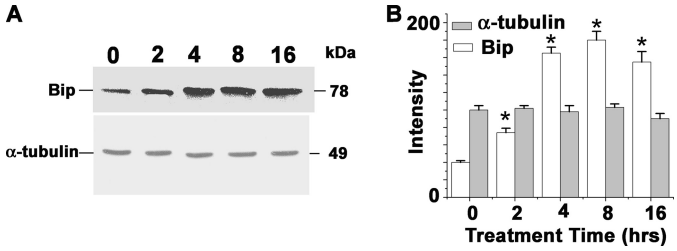

FIGURE 2. **TM induces unfolded protein response in *L. major*.** *A,* Western blot analysis of lysates prepared from DMSO-treated control (*1st lane*) or TM-treated cells (*2nd* to *5th lanes*). 30 μg of total protein was resolved by SDS-PAGE and probed with *T. brucei* anti-Bip antibody or α-tubulin antibody as loading control. The *numbers* on the lanes indicate the hours of treatment. *B,* densitometric analysis of the blot showing up to 4-fold up-regulations of Bip after TM treatment. The *asterisks* indicate the level of statistical significance (0.05).

with DMSO-treated control cells. The DNA fragmentation and PS exposure data were further confirmed by visualizing cells through confocal microscopy (supplemental Fig. S1).

To investigate the possibility that TM induces ER stress and UPR-mediated cell death in *L. major*, we cultured *L. major* cells in the presence of 20 μg/ml TM up to 16 h and analyzed the expression of ER resident chaperone protein Bip/GRP78 as a marker of UPR and ER stress (31). The analysis of Western blot data showed TM-induced marked elevation of Bip/GRP78 expression in a time-dependent manner with a significant rise between 2 and 8 h of treatment (Fig. 2*A*). Densitometric analysis of the Western blot revealed a 4-fold increase in Bip/GRP78 protein expression with respect to control cells (Fig. 2*B*). These results confirmed that TM induced ER stress and consequently terminal UPR gene expression in *L. major* cells.

TM Induces ROS Generation and Cytosolic Ca^{2+} Release in L. major—Prolonged ER stress and UPR contribute to cell death indicating the existence of downstream apoptosis inducing molecules upon TM treatment. Recent studies have suggested ER stress-associated accumulation of endogenous ROS and their involvement in the apoptotic process (19, 32). The association of ER stress and ROS generation was examined with fluorimetric assay of DCFDA up to 1 h. TM treatment showed rapid accumulation of intracellular fluorogenic 2′,7′-dichlorofluorescein indicating generation of ROS. The ROS in TM-treated cells reached a level of 2-fold higher within 1 h (Fig. 3*A*) in comparison with DMSO-treated control cells. Control cells also showed a time-dependent increase in fluorescence intensity probably due to generation of ROS by physiological processes (Fig. 3*A*). To study the involvement of mitochondria in superoxide generation, flow cytometric analysis was performed in the presence of MitoSOX™. Basically, MitoSOX™ is a novel fluorogenic dye for highly selective detection of superoxide in the mitochondria of live cells. The flow cytometric data revealed TM-dependent generation of mitochondrial superoxide in *Leishmania* cells (Fig. 3*B*). To check whether antioxidants eliminate TM-induced ROS generation, we used a well established antioxidant NAC known for its multiple antioxidant properties. Usually NAC is a thiol-containing compound and a precursor of both L-cysteine and reduced glutathione (GSH). NAC maintains reduced intracellular environment by increasing intracellular GSH levels or by serving as a scavenger of H_2O_2, hydroxyl radical, and superoxide. On pretreatment of

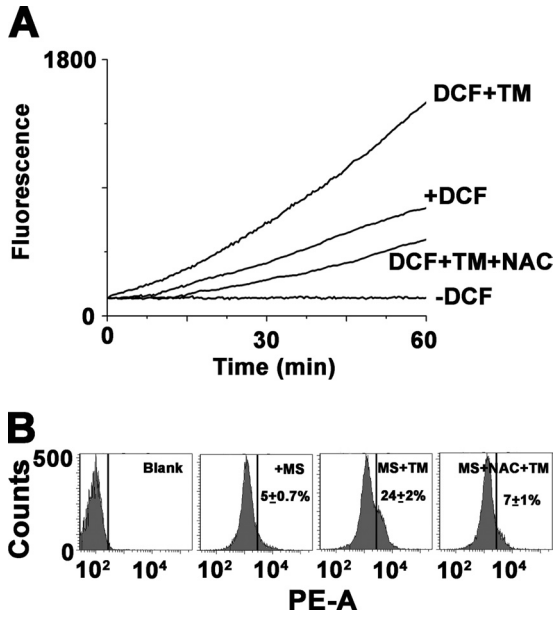

FIGURE 3. **TM induces ROS generation.** *A,* time course kinetic analysis of intracellular ROS generation by H_2DCFDA for the promastigotes treated with 0.2% DMSO alone, 20 μg/ml TM, or after preincubation with NAC. *B,* flow cytometric analysis of mitochondrial ROS generation by MitoSOX™. Data are representative of at least three independent experiments.

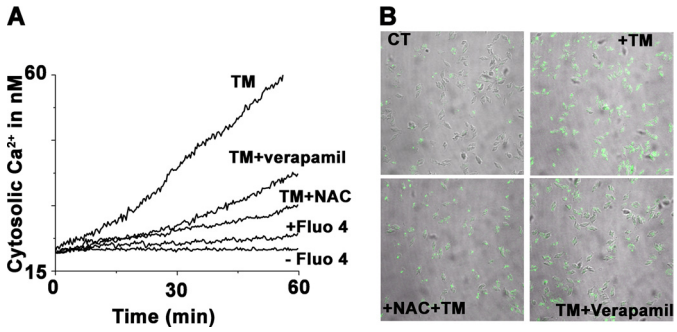

FIGURE 4. **TM induces cytosolic Ca^{2+} release.** *A,* time-dependent intracellular Ca^{2+} release for the promastigotes treated with 0.2% DMSO alone, 20 μg/ml TM, or after preincubation with NAC or verapamil. *B,* increase in Ca^{2+} level as visualized by confocal microscopy. Data are representative of at least three independent experiments.

cells with 20 mM NAC, the generation of both H_2O_2 and superoxide was reduced in TM-treated cells (Fig. 3).

UPR and generation of ROS are associated with the perturbation of cellular Ca^{2+} homeostasis (33). Previous reports on apoptosis in *Leishmania* have shown the release of Ca^{2+} from intracellular stores. As TM treatment induces UPR and ROS generation in *L. major* cells, we wanted to determine whether TM-mediated apoptosis was associated with significant amounts of intracellular calcium release. The presence of free cytosolic calcium was monitored by Ca^{2+}-specific fluorphore Fluo-4/AM whose fluorescence emission increased at 518 nm upon calcium binding. Time-dependent emission kinetics indicate gradual Ca^{2+} accumulation upon TM treatment (Fig. 4*A*). Quantitative and emission intensity analysis showed 3-fold higher levels of cytosolic Ca^{2+} accumulation in TM-treated cells in comparison with control cells (Fig. 4*A*). The involvement of voltage-gated channels and ROS in the delocalization of Ca^{2+} was verified with cells pretreated with the Ca^{2+} channel inhibitor verapamil and the antioxidant NAC. In each case cells showed significantly lesser amount of cytosolic release of calcium (Fig. 4*A*) confirming their role in ER stress-induced Ca^{2+} delocalization in *L. major*. The release of Ca^{2+} was further visualized by confocal microscopy, where higher green fluorescence was seen after TM treatment (Fig. 4*B*).

Generation of ROS and Cytosolic Ca^{2+} Imbalance Induce Mitochondrial Membrane Depolarization and Decline in ATP Production—Intracellular ROS buildup and elevation of cytosolic Ca^{2+} are attributed to mitochondrial dysfunction, which is coupled with a collapse in mitochondrial membrane potential ($\Delta\psi_m$) (34). To examine whether TM induced ROS overload and elevation of cytosolic Ca^{2+} influenced $\Delta\psi_m$ in *L. major,* we measured the $\Delta\psi_m$ by flow cytometry assay using the potentiometric fluorescent dye JC-1. A shift in the fluorescence emission from 530 to 590 nm indicated accumulation of JC-1 in the mitochondria, which was dependent solely on the membrane potential of the mitochondria. Consequently, mitochondrial membrane depolarization was usually accompanied by a decrease in the fluorescence intensity ratio (530 to 590 nm). We observed that incubation with the mitochondrial uncoupler CCCP reduced the JC-1 fluorescence intensity ratio, indicating that the JC-1 response in *Leishmania* cells was sensitive to changes in membrane potential (Fig. 5*A*). Treatment with tunicamycin resulted in gradual depolarization (Fig. 5*B*), which was indicated by decreasing the fluorescence intensity ratio (590/530 nm). Pretreatment of cells with antioxidant NAC and depletion of free cytosolic Ca^{2+} by blocking intracellular voltage-gated channel with verapamil showed protection in $\Delta\psi_m$ decline, indicating the potential role of ROS and Ca^{2+} in TM-induced mitochondrial membrane depolarization.

The ATP level is an important factor, as progression to necrosis or apoptosis depends on the availability of ATP (35). We measured the ATP content in TM-treated parasites to determine whether the breakdown in mitochondrial function correlated with the decline in the production of ATP. TM treatment caused a gradual fall in the ATP levels. Total cellular ATP was ~4-fold lower in TM-treated parasites than DMSO-treated parasites (Fig. 5*C*). Furthermore, the preservation of total cellular ATP content was observed in NAC- or verapamil-pretreated cells (Fig. 5*C*).

TM Promotes Cyt C and Endo G Release from Mitochondria and Subsequent Translocation of Endo G to Nucleus—Oxidative stress and imbalance in cytosolic and mitochondrial Ca^{2+} overload promote release of mitochondrial resident apoptotic factors like Cyt *c*, apoptosis-inducing factor, and Endo G, which play crucial roles in downstream apoptotic processes (36). Cytochrome *c* acts as a component of the apoptosome complex that promotes activation of nascent caspase after its release in cytosol (37). Endo G is a mitochondrial nuclease that has been suggested to play a role in mitochondrial DNA replication (38), and its role in nuclear DNA fragmentation during apoptosis has been evidenced from the studies on *Caenorhabditis elegans* (39, 40). The release of Endo G from mitochondria and its translocation to nuclei have been documented in different cell lines during apoptotic stimuli (41–43). In *Leishmania,* both Cyt *c* and Endo G have been reported to play important roles in apoptosis (6). The mitochondrial release of Endo G and its involve-

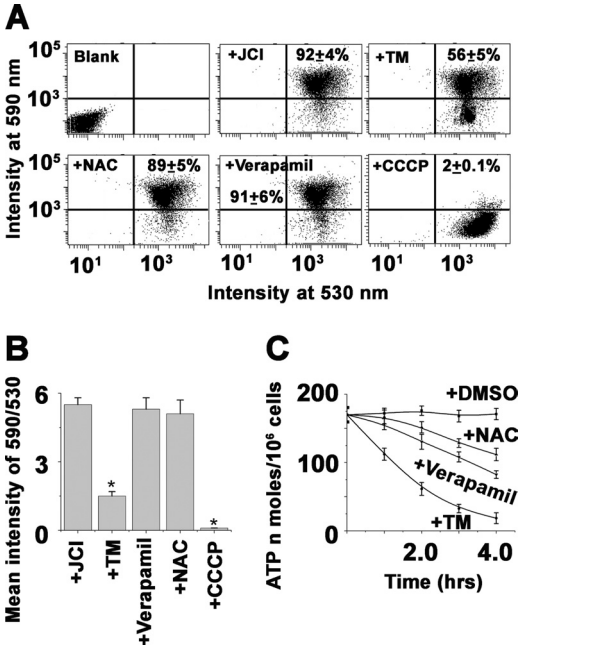

FIGURE 5. **Effect of ER stress on the $\Delta\Psi_m$ in *L. major*.** *L. major* cells (10^7/ml) were incubated with the potential sensitive probe JC-1 (6 μM) for 15 min at 25 °C to assess $\Delta\Psi_m$ after treatment with 0.2% DMSO or TM (20 μg/ml) and analyzed by flow cytometry with excitation at 488 nm. Emission was detected at 530 nm for monomer and 590 nm for J-aggregate. A drop in $\Delta\Psi_m$ was identified as a change in JC-1 properties from forming J-aggregates (emission at 590 nm) at high $\Delta\Psi_m$ to forming J-monomers (emission at 530 nm) at low $\Delta\Psi_m$. The nearly complete monomer was induced by treating cells with 50 μM CCCP, an uncoupler of mitochondrial respiration, 15 min prior to addition of JC-1. *Blank* in dot plots indicates blank cells (cells without JC-1); +*JC1* indicates 0.2% DMSO-treated cells stained with JC-1 as control; +*TM* indicates 8-h TM-treated JC-1-stained cells; +*NAC* indicates NAC-preincubated and 8-h TM-treated JC-1-stained cells; +*Verapamil* indicates verapamil-preincubated, 8-h TM-treated JC-1-stained cells, and +*CCCP* indicates CCCP-treated JC-1-stained cells. Data are representative of at least three independent experiments. *B,* time-dependent analysis of 590/530 values of DMSO-treated control cells, cells treated with 20 μg/ml TM, cells preincubated with NAC and Ca^{2+} channel inhibitor verapamil, and cells treated with CCCP. Data are representative of means ± S.D. of three independently performed experiments. The *asterisks* indicate the level of statistical significance (0.05). *C,* time-dependent measurement of intracellular ATP levels in DMSO-treated control cells and cells treated with TM or TM-treated but preincubated with NAC and verapamil. ATP concentration is expressed as nanomoles of ATP/10^6 cells. Values were average ± S.D. of three independent experiments.

ment in DNA fragmentation have also been shown in kinetoplastid parasites during oxidative stress-induced apoptosis (8, 44). Subcellular fractionation and Western blot analysis were performed to check the possibility of TM-induced release of cytochrome *c* and Endo G from mitochondria. Immunoblot data revealed time-dependent cytosolic accumulation of both Cyt *c* and Endo G from mitochondria (Fig. 6). Significant amount of Endo G was detected in nuclear fractions after TM treatment (Fig. 6). However, critical analysis of the data revealed that both Cyt *c* and Endo G translocation from mitochondria were prevented by NAC pretreatment, suggesting TM-induced Cyt *c* and Endo G release from mitochondria was due to elevated levels of oxidative stress. As control markers for mitochondria, cytoplasm, and nucleus, we used the mitochondrial RNA import complex-I, cytosolic adenosine kinase, and nuclear histone H3B, respectively.

Measurement of Caspase-like Protease Activity—Caspases are cysteine proteases, which play an important role in ER stress-induced apoptosis (45–47). To check whether ER stress activates caspase-like protease in *L. major*, we measured caspase-12, caspase-3/7, and metacaspase-like protease activity after treatment of TM for 16 h. Caspase-3/7-like activity was measured by flow cytometry using fluorogenic caspase-3/7 inhibitor FAM-DEVD-FMK. Caspase-12-like protease activity was measured based on detection of cleavage of substrate ATAD-AFC by fluorescence plate reader as described under "Experimental Procedures." For inhibition study, Z-VAD-FMK and Z-ATAD-FMK were used as specific inhibitors of caspase-3/7 and caspase-12, respectively. Table 1 data showed that only the basal level of caspase-12-like activity was detected, which was not increased significantly throughout the study period. However, TM-treated cells showed a 1.5-fold higher caspase-3/7-like activity compared with control cells. This increased activity was inhibited by caspase inhibitor Z-VAD-FMK. Recently, a group of workers has reported about metacaspase genes in *Leishmania*; these are efficiently able to cleave trypsin substrates and are unable to cleave caspase-specific substrates. Consistently, that activity is insensitive to caspase inhibitors and is efficiently inhibited by trypsin inhibitors, such as antipain (29). To check whether control cells show any difference in metacaspase-like activity in the presence of TM, we used the *Leishmania* metacaspase-specific fluorogenic substrate, Boc-GRR-AMC. The metacaspase-like activity upon TM treatment in comparison with basal level as obtained in DMSO-treated control cells was only 1.6-fold higher (Table 1) and that changing activity of TM-treated cells was inhibited by antipain. Thus, these results indicated that the TM was able to induce ~1.5-fold in both caspase-3/7 and metacaspase-like activity in *Leishmania*.

TM-mediated Apoptosis of L. major Is Caspase-independent—Release of mitochondrial apoptotic factors suggests their possible role in the apoptotic pathway. A growing body of evidence indicated that *Leishmania,* like multicellular organisms, undergoes apoptosis through both caspase-dependent and -independent pathways (8–10). Flow cytometric analysis of phosphatidylserine exposure in the presence of caspase inhibitor Z-VAD-FMK or metacaspase inhibitor antipain showed their inability to prevent apoptosis. Rather pretreatment of cells with NAC, GSH, and L-cysteine or intracellular Ca^{2+} chelator BAPTA-AM showed efficient apoptosis inhibition (Fig. 7*A*). These results indicated that TM-induced phosphatidylserine exposure was a caspase-independent phenomenon, although it was clear that oxidative stress and elevated levels of cytosolic Ca^{2+} played a crucial role in ER stress-induced phosphatidylserine exposure of *L. major*. Similarly, DNA fragmentation assay by TUNEL assay showed 10% protection by Z-VAD-FMK or antipain but about 80% protection was found in cells pretreated with NAC, GSH, L-cysteine, or BAPTA-AM (Fig. 7*B*).

Chemical chaperone, such as PBA, is a low molecular weight compound known to stabilize protein conformation, improve ER folding capacity, and facilitate the trafficking of mutant proteins (48, 49). To investigate the action of chemical chaperone, we first tested whether PBA protected against TM-induced ER stress as well as DNA fragmentation and PS externalization in *Leishmania*. Pretreatment of *Leishmania* cells with 2.0 mM PBA suppressed TM-induced DNA fragmentation and PS

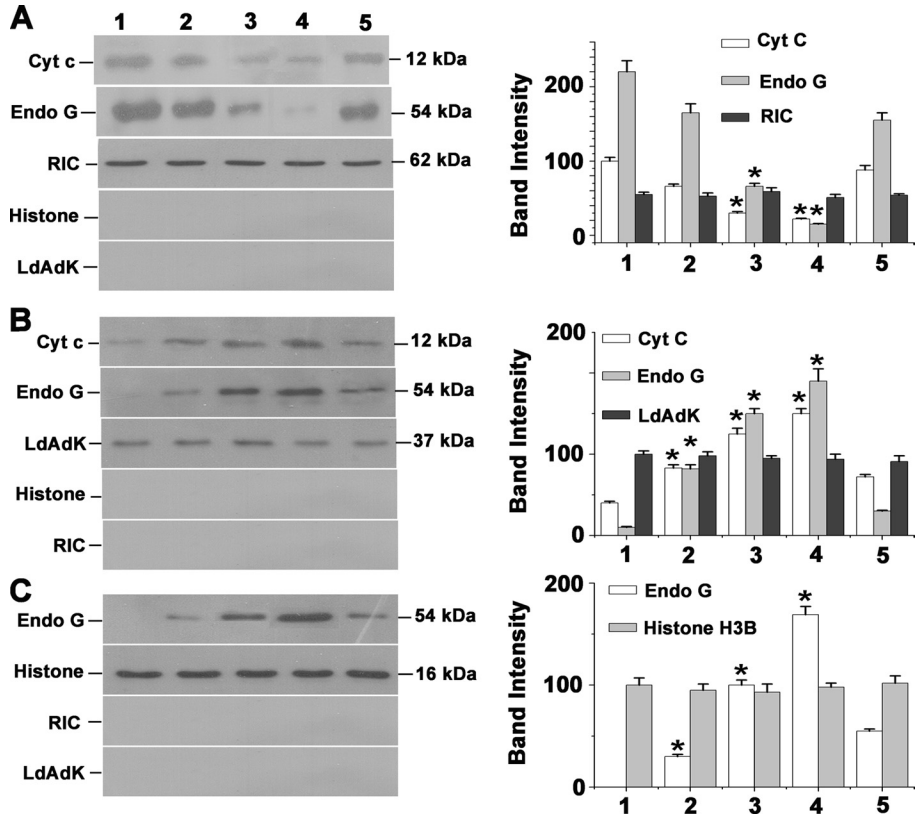

FIGURE 6. **TM induces Cyt *c* and Endo G release from mitochondria to cytosol and translocation of Endo G from cytosol to nucleus.** *A,* Western blot analysis of Cyt *c* and Endo G in mitochondrial fraction of 0.2% DMSO-treated control and TM (20 μg/ml)-treated cells. *Lane 1* represents DMSO-treated control. *Lanes 2–4* indicate cells treated with TM for 2, 4, and 8 h, respectively. *Lane 5* denotes pretreatment with NAC before treatment with TM for 8 h. *B,* Western blot analysis of Cyt *c* and Endo G in cytosolic fraction. *C,* immunoblot analysis of Endo G in nuclear fractions of control (0.2% DMSO-treated) and TM-treated cells. All the data are representative of at least three independent experiments. The *asterisks* indicate the level of statistical significance (0.05). *RIC*, mitochondrial RNA import complex I; *LdAdK*, *L. donovani* adenosine kinase. * indicates the level of statistical significance (0.05).

TABLE 1

Measurement of caspase-like activity in control and TM-treated *L. major* cells

An increased fluorescence intensity indicates increased caspase-like protease activity. Measurements were described under "Experimental Procedures." Each value represents the means ± S.D. for three independent experiments. FLICA indicates a caspase-3- and -7-specific fluorogenic inhibitor.

	Caspase-12-like activity		Caspase 3/7-like activity		Metacaspase-like activity	
Cells	ATAD-AFC	ATAD-AFC and Z-ATAD-FMK	FLICA	FLICA and VAD-FMK	Boc-GRR-AMC	Boc-GRR-AMC and antipain
Control	18757 ± 1578	18353 ± 1218	162 ± 11	122 ± 14	409 ± 30	338 ± 29
TM treated	21676 ± 1131	19912 ± 2078	231 ± 17	176 ± 9	658 ± 21	425 ± 32

externalization (Fig. 7) confirming the involvement of ER stress in TM-treated cell death.

DISCUSSION

In this study, we have addressed the molecular mechanisms of prolonged ER stress-mediated apoptosis in *Leishmania* cells by using antibiotic TM, which prevents the naturally occurring *N*-glycosylation of protein in ER. Our findings on Bip expression indicate that TM treatment exhibits UPR activation in *Leishmania*. We show for the first time that TM-induced apoptosis in *Leishmania* is due to the rapid accumulation of ROS and intracellular release of Ca^{2+} following ER stress, and it is abolished by the use of antioxidants, such as NAC and Ca^{2+} chelators, like BAPTA-AM.

In multicellular organisms, two mechanisms apparently operate independent of one another in ER stress-induced apoptosis (45–47). One is a mitochondrial dependent apoptotic pathway, and the second is a caspase-12-dependent apoptotic pathway (47). The negative assays for caspase-12-like protein (Table 1) and ineffectiveness of Z-VAD-FMK to prevent DNA degradation suggest that ER stress-induced apoptosis in *Leishmania* occurs through a caspase-12-independent apoptotic pathway. Therefore, it must be the other option that is responsible for in ER stress-induced apoptosis in *Leishmania*. Evidence suggests that ER stress agents cause loss of mitochondrial transmembrane potential and promote mitochondrial release of Cyt *c* (45, 50), leading to cellular apoptosis via caspase-dependent or caspase-independent pathways. In general, the generation of ROS through oxidative protein folding (19) and perturbation of intracellular Ca^{2+} are found during ER stress-mediated apoptosis (33). Our experiments using antioxidants and Ca^{2+} chelator further indicate that both ROS generation and perturbations of intracellular Ca^{2+} level act upstream of

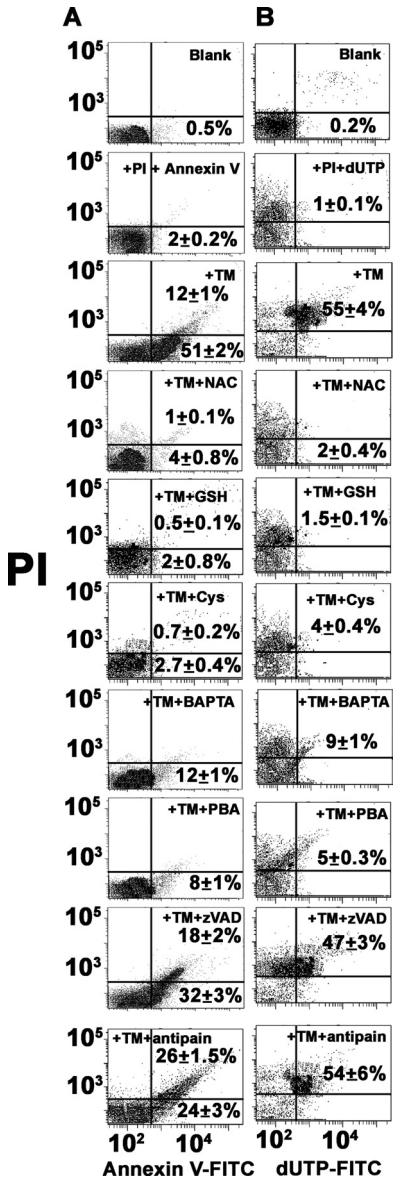

FIGURE 7. **Analysis of ER stress-induced apoptosis in *L. major* in presence of different inhibitors.** *A,* flow cytometric analysis of PS exposure in DMSO-treated control cells, 16 h in TM-treated cells, and cells pretreated with NAC, GSH, L-cysteine, BAPTA-AM, PBA (chemical chaperone), antipain, and Z-VAD-FMK. *Lower right* and *upper right quadrants* of each dot plot represent apoptotic cells. *B,* flow cytometric analysis of DNA fragmentation by TUNEL assay. *Lower right* and *upper right quadrants* of each dot plot represent TUNEL-positive apoptotic cells. Data are representative of three independent experiments.

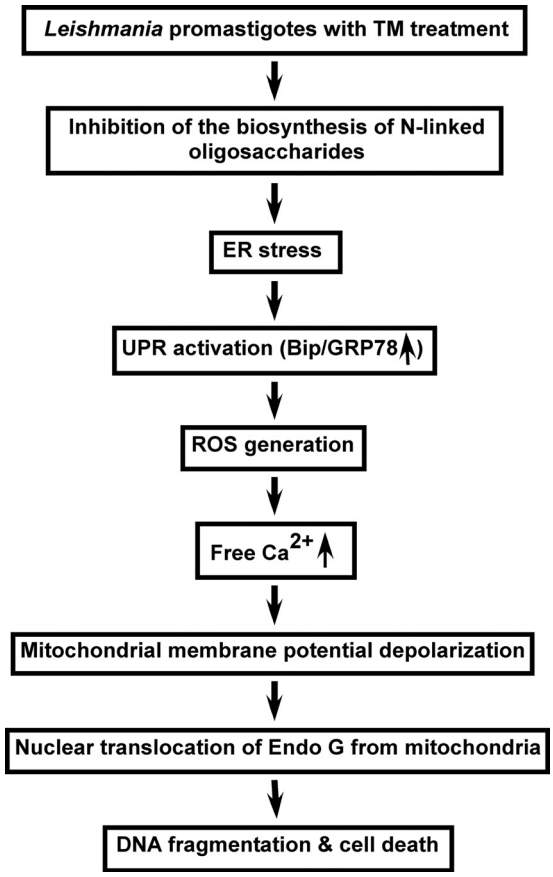

FIGURE 8. **Schematic diagram of TM-induced ER-stress in *Leishmania* leading to caspase-independent programmed cell death.**

mitochondrial depolarization. Eventually, we observed in *Leishmania* cells that NAC substantially inhibited ROS production and simultaneously prevented both the elevation of Ca^{2+} levels and disruption of the mitochondrial depolarization ($\Delta\Psi_m$) after treatment with TM. Thus, ROS production in TM-induced *Leishmania* cells acts upstream of the Ca^{2+} release from the internal store to cytosol. TM-induced mitochondrial depolarization in *Leishmania* is also protected by chelation of free Ca^{2+}. Therefore, the intracellular Ca^{2+} level acts upstream of mitochondrial depolarization.

Although both caspase-dependent and caspase-independent pathways of apoptosis have been studied in *Leishmania*, the main question centers round the mechanism of apoptosis triggered by ER stress in *Leishmania.* Depolarization of mitochondria causes the release of proapoptotic molecules such as Cyt *c*, Endo G, and apoptosis-inducing factor (51). From our results on the basis of subcellular fractionation and Western blot, the nuclear localization of Endo G is detected in TM-treated apoptotic *Leishmania* cells. Several groups established that Endo G acts as an apoptotic DNase when released from the mitochondria to the nucleus (8, 40, 44). Preincubation with Z-VAD-FMK (caspase inhibitor) or antipain (*Leishmania* metacaspase inhibitor) cannot inhibit DNA fragmentation and PS externalization in TM-treated apoptotic *Leishmania* cells, although caspase or metacaspase-like activity is ~1.5-fold higher after 16 h of treatment with TM. Thus, these results strongly suggest that caspase-independent cell death in TM-treated *Leishmania* is considered to be mediated by the nuclear translocation of the mitochondrial DNA repair enzyme (Endo G).

Thus, apoptosis in ER stress-induced *Leishmania* is mediated by the mitochondrial apoptotic pathway involving ROS production, cytosolic Ca^{2+} imbalance, mitochondrial depolarization, and ultimately release of Endo G from mitochondria to the nucleus via cytoplasm. Based on the sequence of our results, Fig. 8 represents a proposed pathway in TM-induced *Leishmania* cell death. It is confirmed from our results that the step at the very beginning of ER stress-induced apoptosis in *Leishmania* involves the generation of ROS. How ER stress produces ROS in *Leishmania* remains unclear. Recently, Goldshmidt *et*

al. (52) has proposed that persistent ER stress induces the spliced leader RNA silencing pathway, leading to programmed cell death in *T. brucei*. In multicellular organisms, ER oxidoreductin (Ero1p) and protein-disulfide isomerase (Pdi1p) act in concert, during the formation of disulfide bonds in the ER, to transfer electrons from the thiol groups of substrate proteins to molecular oxygen with the generation of ROS as a by-product (19). Although the putative protein sequences of Ero1p (Gene Bank accession number CAJ 04154) and Pdi1p (Gene Bank accession number CAJ04838) are present in the *Leishmania* genome, it is completely unknown whether those genes have any role in ER stress-induced ROS production. The knock-out result of the two genes will be helpful in elucidating the exact molecular mechanisms of ER stress-induced ROS generation in *Leishmania* in the near future.

Acknowledgments—We thank Alok. K. Datta for L. donovani adenosine kinase antibody; Hemanta K. Majumder for L. donovani endonuclease G antibody; Samit Adhya for mitochondrial RNA import complex I antibody; James D. Bangs (University of Wisconsin, Madison) for T. brucei Bip antibody, and Andre Schneider (University of Berne, Switzerland) for T. brucei cytochrome c antibody.

REFERENCES

1. van Zandbergen, G., Bollinger, A., Wenzel, A., Kamhawi, S., Voll, R., Klinger, M., Müller, A., Hölscher, C., Herrmann, M., Sacks, D., Solbach, W., and Laskay, T. (2006) *Proc. Natl. Acad. Sci. U.S.A.* **103,** 13837–13842
2. Pal, S., Dolai, S., Yadav, R. K., and Adak, S. (2010) *PLoS One* **5,** e11271
3. van Zandbergen, G., Solbach, W., and Laskay, T. (2007) *Autoimmunity* **40,** 349–352
4. Sudhandiran, G., and Shaha, C. (2003) *J. Biol. Chem.* **278,** 25120–25132
5. Das, M., Mukherjee, S. B., and Shaha, C. (2001) *J. Cell Sci.* **114,** 2461–2469
6. Sen, N., Das, B. B., Ganguly, A., Mukherjee, T., Tripathi, G., Bandyopadhyay, S., Rakshit, S., Sen, T., and Majumder, H. K. (2004) *Cell Death Differ.* **11,** 924–936
7. Kulkarni, M. M., McMaster, W. R., Kamysz, W., and McGwire, B. S. (2009) *J. Biol. Chem.* **284,** 15496–15504
8. BoseDasgupta, S., Das, B. B., Sengupta, S., Ganguly, A., Roy, A., Dey, S., Tripathi, G., Dinda, B., and Majumder, H. K. (2008) *Cell Death Differ.* **15,** 1629–1640
9. Arnoult, D., Akarid, K., Grodet, A., Petit, P. X., Estaquier, J., and Ameisen, J. C. (2002) *Cell Death Differ.* **9,** 65–81
10. Zangger, H., Mottram, J. C., and Fasel, N. (2002) *Cell Death Differ.* **9,** 1126–1139
11. Kaufman, R. J. (2002) *J. Clin. Invest.* **110,** 1389–1398
12. Rutkowski, D. T., and Kaufman, R. J. (2004) *Trends Cell Biol.* **14,** 20–28
13. Boyce, M., and Yuan, J. (2006) *Cell Death Differ.* **13,** 363–373
14. Ron, D. (2002) *J. Clin. Invest.* **110,** 1383–1388
15. Oyadomari, S., Araki, E., and Mori, M. (2002) *Apoptosis* **7,** 335–345
16. Zhang, K., and Kaufman, R. J. (2004) *J. Biol. Chem.* **279,** 25935–25938
17. Paz Gavilán, M., Vela, J., Castaño, A., Ramos, B., del Río, J. C., Vitorica, J., and Ruano, D. (2006) *Neurobiol. Aging* **27,** 973–982
18. Haynes, C. M., Titus, E. A., and Cooper, A. A. (2004) *Mol. Cell* **15,** 767–776
19. Tu, B. P., and Weissman, J. S. (2004) *J. Cell Biol.* **164,** 341–346
20. Elbein, A. D. (1987) *Annu. Rev. Biochem.* **56,** 497–534
21. Dricu, A., Carlberg, M., Wang, M., and Larsson, O. (1997) *Cancer Res.* **57,** 543–548
22. Delom, F., Emadali, A., Cocolakis, E., Lebrun, J. J., Nantel, A., and Chevet, E. (2007) *Cell Death Differ.* **14,** 586–596
23. Kink, J. A., and Chang, K. P. (1987) *Proc. Natl. Acad. Sci. U.S.A.* **84,** 1253–1257
24. Dagger, F., Ayesta, C., and Hernandez, A. G. (1984) *Biol. Cell* **50,** 173–189
25. Nolan, T. J., and Farrell, J. P. (1985) *Mol. Biochem. Parasitol.* **16,** 127–135
26. Dolai, S., Yadav, R. K., Pal, S., and Adak, S. (2008) *Free Radic. Biol. Med.* **45,** 1520–1529
27. Dolai, S., Yadav, R. K., Pal, S., and Adak, S. (2009) *Eukaryot. Cell* **8,** 1721–1731
28. Adak, S., and Datta, A. K. (2005) *Biochem. J.* **390,** 465–474
29. Lee, N., Gannavaram, S., Selvapandiyan, A., and Debrabant, A. (2007) *Eukaryot. Cell* **6,** 1745–1757
30. Moss, C. X., Westrop, G. D., Juliano, L., Coombs, G. H., and Mottram, J. C. (2007) *FEBS. Lett.* **581,** 5635–5639
31. Lee, A. S. (2005) *Methods* **35,** 373–381
32. Chae, H. J., Kim, H. R., Xu, C., Bailly-Maitre, B., Krajewska, M., Krajewski, S., Banares, S., Cui, J., Digicaylioglu, M., Ke, N., Kitada, S., Monosov, E., Thomas, M., Kress, C. L., Babendure, J. R., Tsien, R. Y., Lipton, S. A., and Reed, J. C. (2004) *Mol. Cell* **15,** 355–366
33. Deniaud, A., Sharaf el dein, O., Maillier, E., Poncet, D., Kroemer, G., Lemaire, C., and Brenner, C. (2008) *Oncogene* **27,** 285–299
34. Balaban, R. S., Nemoto, S., and Finkel, T. (2005) *Cell* **120,** 483–495
35. Lemasters, J. J., Qian, T., Bradham, C. A., Brenner, D. A., Cascio, W. E., Trost, L. C., Nishimura, Y., Nieminen, A. L., and Herman, B. (1999) *J. Bioenerg. Biomembr.* **31,** 305–319
36. Green, D. R., and Kroemer, G. (2004) *Science* **305,** 626–629
37. Li, P., Nijhawan, D., Budihardjo, I., Srinivasula, S. M., Ahmad, M., Alnemri, E. S., and Wang, X. (1997) *Cell* **91,** 479–489
38. Côté, J., and Ruiz-Carrillo, A. (1993) *Science* **261,** 765–769
39. Parrish, J., Li, L., Klotz, K., Ledwich, D., Wang, X., and Xue, D. (2001) *Nature* **412,** 90–94
40. Li, L. Y., Luo, X., and Wang, X. (2001) *Nature* **412,** 95–99
41. van Loo, G., Schotte, P., van Gurp, M., Demol, H., Hoorelbeke, B., Gevaert, K., Rodriguez, I., Ruiz-Carrillo, A., Vandekerckhove, J., Declercq, W., Beyaert, R., and Vandenabeele, P. (2001) *Cell Death Differ.* **8,** 1136–1142
42. Ishihara, Y., and Shimamoto, N. (2006) *J. Biol. Chem.* **281,** 6726–6733
43. Strauss, G., Westhoff, M. A., Fischer-Posovszky, P., Fulda, S., Schanbacher, M., Eckhoff, S. M., Stahnke, K., Vahsen, N., Kroemer, G., and Debatin, K. M. (2008) *Cell Death Differ.* **15,** 332–343
44. Gannavaram, S., Vedvyas, C., and Debrabant, A. (2008) *J. Cell Sci.* **121,** 99–109
45. Häcki, J., Egger, L., Monney, L., Conus, S., Rossé, T., Fellay, I., and Borner, C. (2000) *Oncogene* **19,** 2286–2295
46. Nakagawa, T., and Yuan, J. (2000) *J. Cell Biol.* **150,** 887–894
47. Nakagawa, T., Zhu, H., Morishima, N., Li, E., Xu, J., Yankner, B. A., and Yuan, J. (2000) *Nature* **403,** 98–103
48. Ozcan, U., Yilmaz, E., Ozcan, L., Furuhashi, M., Vaillancourt, E., Smith, R. O., Görgün, C. Z., and Hotamisligil, G. S. (2006) *Science* **313,** 1137–1140
49. Datta, R., Waheed, A., Shah, G. N., and Sly, W. S. (2007) *Proc. Natl. Acad. Sci. U.S.A.* **104,** 19989–19994
50. Boya, P., Cohen, I., Zamzami, N., Vieira, H. L., and Kroemer, G. (2002) *Cell Death Differ.* **9,** 465–467
51. Atlante, A., Calissano, P., Bobba, A., Azzariti, A., Marra, E., and Passarella, S. (2000) *J. Biol. Chem.* **275,** 37159–37166
52. Goldshmidt, H., Matas, D., Kabi, A., Carmi, S., Hope, R., and Michaeli, S. (2010) *Plos Pathog.* **6,** e1000731